Ultrasonic Guided Waves-Based Nonlinear Autoregressive Defect Detection for Railway Tracks Using Fiber Bragg Grating Sensing

DA-ZHI DANG, YOU-WU WANG and YI-QING NI

ABSTRACT

Structural health monitoring (SHM) is crucial to the maintenance and daily operation of civil infrastructures. Railway system, which plays an important role in modern society, relies heavily on robust monitoring systems to give timely warnings of early-stage defects that potentially could result in the consequences of major traffic incidents, such as derailments. Guided wave testing (GWT) methods have been introduced into the rail track monitoring, featuring long-distance monitoring reliability, high sensitivity, and excellent efficiency. In recent yea rs, the deployment of optical fiber-based GWT on railway system has prevailed traditional piezoelectric sensing-based schemes, due to its reliable performance especially under high electromagnetic interference (EMI) environments. In this paper, experimental studies are conducted, where fiber Bragg grating (FBG) sensors are utilized to receive ultrasonic guided waves (UGWs) on railway tracks, induced by a lead zirconate titanate (PZT) sensor, to detect defects. A narrow-band laser is induced to conduct edge filter demodulation of ultrasonic FBGs, with the sampling frequency of 10 MHz. A nonlinear autoregressive neural network with exogenous inputs (NARX) is trained using the acquired UGW signals and is utilized to evaluate rail track condition by extracting damage sensitive features (DSFs) based on the probabilistic density function (PDF) of the prediction error. First, a DSF baseline is obtained using the UGW data acquired from an intact rail track; then, for an unknown rail condition, the signals are processed by the trained NARX model to calculate DSFs; by comparing the calculated DSFs with the baseline, the rail condition can be evaluated. In this research, various UGW excitation frequencies are deployed, and for each frequency band an individual NARX model is trained. The prediction results show that the proposed method is highly sensitive to rail cracks, with an obvious increase in DSF values when an artificial crack is placed, which denotes the promising application of this method into SHM for mass rail transit systems.

Da-Zhi Dang, You-Wu Wang, Yi-Qing Ni, Department of Civil and Environmental Engineering, The Hong Kong Polytechnic University, Hung Hom, Kowloon, Hong Kong S.A.R., China

INTRODUCTION

The maintenance of modern civil infrastructures has been extensively researched through the past decades, ensuring that major incidents can be prevented. It has been repeatedly reported that most of the railway failures are the consequence of railway track damages, such as fatigue cracks and weld defects. Therefore, a reliable SHM system designed to detect rail track damages is required to rule out potential risks of failure.

Guided wave testing (GWT) is an important branch of non-destructive evaluation (NDE) technique [1], which has been deployed to damage detection of railway tracks. Such method has attained growing attention, due to its rapid and accurate inspection performance, non-destructive characteristic, and high sensitivity to minor damages [2]. In a normal procedure of the GWT-based damage detection process, ultrasonic guided waves (UGWs) are actively induced via either contact or non-contact sensors and are received by transducers. This testing procedure can be repeatedly carried out, depending on the specifically designated monitoring period, generally with the advantages of long range, flexible distance and high reliability and durability, compared to traditional bulk wave testing (BWT) methods. More importantly, high-frequency UGW is damage-sensitive when it comes to railway defects, such as fatigue cracks [3]. However, the quality of the UGW signals can be compromised due to the electromagnetic interference (EMI) on railway sites. To this regard, optical acoustic sensing has been introduced to the monitoring of railway tracks considering its non-electric characteristic and high endurance in ambient EMI [4][5]. Compared to traditional piezoelectric material-made sensors, fiber Bragg grating (FBG) sensors are not only capable of performing in harsh railway environments, but also are considered economically efficient because of the low costs for production and maintenance of optical fibers [6].

The propagation of UGWs in railway tracks has been researched. It has been concluded in literature that the complex boundary conditions of the rail track result in highly non-linear signals due to multiple reflections and scatterings [3][5][7][8]. Therefore, instead of analyzing the time-domain series which is a common solution for Lamb wave-based damage detection [9], it is generally difficult to extract useful information from the raw signals collected from a railway track. Consequently, energy-based damage index is proposed, representing the possible energy loss when the UGWs encounter a barrier, e.g., a crack or a weld. Apart from that, time and frequency domain parameters are also extracted to study the propagation of UGWs [10][11]. In recent years, with the growing trend of using efficient machine learning algorithms to extract features and process signals, various neural network structures have been proposed to process the time series. The autoregressive (AR) model and autoregressive model with exogenous inputs (ARX) are commonly used when processing the structural dynamic responses, such as accelerations and displacements, in SHM [12][13]. To deploy time-series-based models into processing UGW signals that propagate in rail tracks where nonlinear boundary conditions are considered, it is intuitive to apply a nonlinear model with more robust fitting performance. Nonlinear autoregressive model with exogenous inputs (NARX), proved to be capable of performing system identification in various fields [14], is deployed in this paper. The multi-input characteristics of the NARX makes it a powerful tool when applied to processing multi-channel signals of a sensor network with complex nonlinear relations.

In this paper, a NARX-based damage detection framework is proposed to conduct NDE on rail tracks using FBG. A probabilistic damage sensitive feature (DSF) is also developed for damage diagnosis. Experimental studies are conducted to verify the feasibility of the proposed method, where an artificial crack is created on the rail web. Then, NARX models are constructed and trained on the UGW signals collected, with varying frequency bands. The DSFs are calculated for both the intact and defected rail conditions. In the following contents, the damage detection methodology and the experimental setup are introduced in Section 2 and 3, respectively. Last, the results of the proposed NARX-based damage detection method are shown in Section 4, where further discussions are also included.

NARX-BASED DAMAGE DETECTION

NARX Neural Networks

For a typical multi-input single-output (MISO) system, the autoregression model F can be formatted as,

$$\hat{y}(t) = F[b_0 + \sum_{h=1}^{Nh} W_{h0} \cdot f_h(b_h + \sum_{i=1}^{d_x} W_{ih} x(t-i) + \sum_{j=1}^{d_y} W_{jh} y(t-j))] \quad (1)$$

where y and $\hat{y}$ are the original and predicted targets, respectively; x denotes the input time-series; d_x and d_y refer to the time delays of the exogenous input and the target; W_h and b_h are weights and the bias matrixes of the hidden layers. The dimension of the exogenous matrix x is determined by the number of inputs and the length of the signals. With F representing the nonlinear function, f being the activation function of the neurol nodes, usually being sigmoid or SoftMax, Equation 1 can be regarded as the basic format of a NARX model.

Damage Sensitive Feature

After constructing a robust nonlinear regressor, it is vital that suitable damage sensitive features (DSFs) are extracted based on the regression results [15]. In this paper, a probability density function (PDF) based DSF format is adopted to represent the damage status of the rail tracks.

It is assumed that the prediction error of a NARX neural network should approximate to a Gaussian distribution. Therefore, the following equation can be obtained,

$$G(e) = \frac{1}{\sigma\sqrt{2\pi}} \exp\left[-\frac{(e-\mu)^2}{2\sigma^2}\right] \quad (2)$$

where e denotes the prediction error vector of the NARX; μ and σ are the mean value and the standard deviation of the distribution. After obtaining a baseline distribution $G_b(e_b)$ through the NARX trained with the datasets collected whilst the rail track is under healthy condition, the prediction error distribution of the data of an unknown condition $G_u(e_u)$ is utilized for comparison, to determine whether the rail track condition is close to that of the baseline condition. The DSF deployed in this paper is formatted via the following equation,

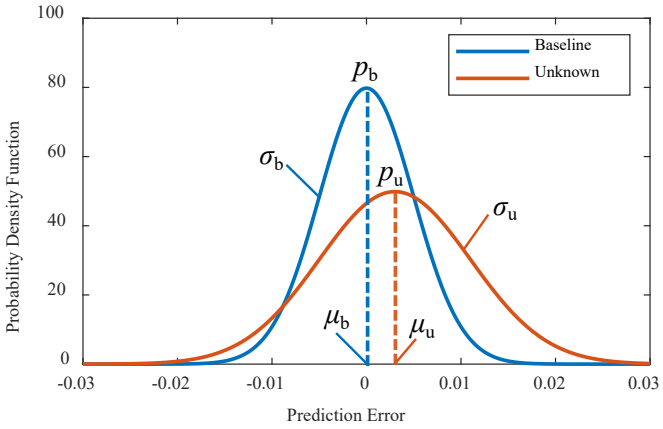

Figure 1. Extracting damage-sensitive features from a typical PDF.

$$DSF = \log\left(\frac{\sigma_u p_b}{\sigma_b p_u} + 1\right) \tag{3}$$

where p_b, p_u are the peak values of the PDFs of the baseline and the unknown conditions, respectively. To thoroughly demonstrate the concept of the Equation 3, a schematic is given in Figure 1 where two PDF curves are drawn to show the features extraction process. Equation 3 can accurately describe the difference between the PDFs of the baseline and an unknown condition.

EXPERIMENTAL SETUP

The schematic of the experimental setup is shown in Figure 2. The computer-based controlling instrument (PXI-5412, produced by National Instruments, Austin, TX, USA) is composed of 2 main parts, an arbitrary generator, and a digital oscilloscope respectively. The electric signals generated are transmitted to the power amplifier (HVA-400-A, produced by Ciprian, Grenoble, France). The UGWs are induced using a lead zirconate titanate (PZT) based sensor. When transmitting a 5-cycle sinusoidal tone voltage pulses modulated by a Hanning Window into the PZT, the material vibrates accordingly.

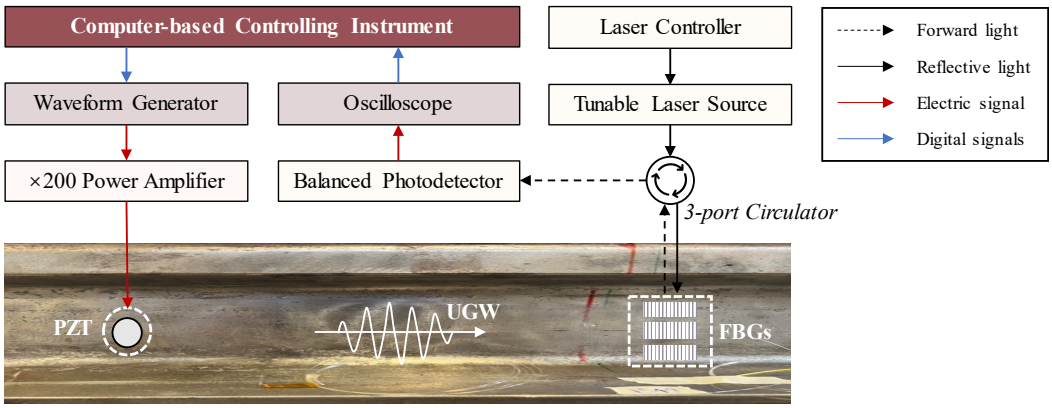

Figure 2. Schematic of the experimental setup.

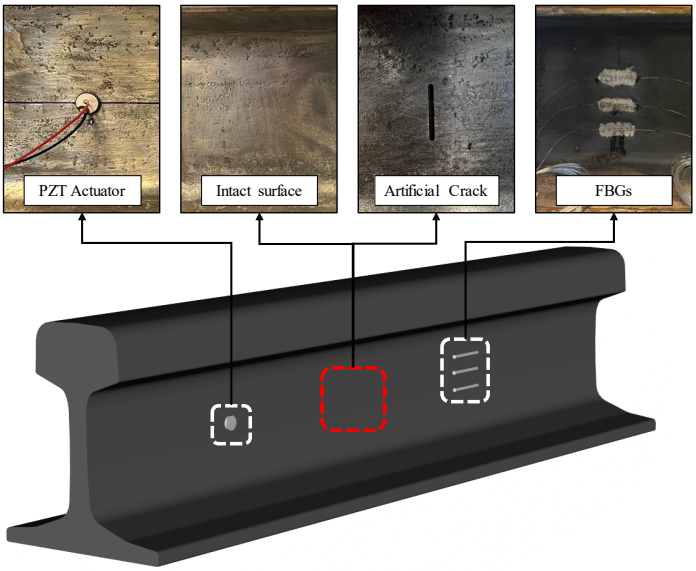

Figure 3. UGW transducing configurations and rail conditions considered.

The demodulation of the FBG is based on edge filter technique. A narrow-bandwidth light with a central frequency range that meets the 3-dB point of an FBG is emitted from a tunable laser source (TLB-6700, produced by Newport, Irvine, CA, USA). The grating length of the FBG is 10 mm and the Bragg wavelength is 1560 nm in this case. The grating area is glued to the rail web via adhesives. The reflected light is converted into electrical signals through a balanced photodetector (2117-FC, produced by Newport, Irvine, CA, USA) and then the signals are recorded by the computer-based controlling instrument. The UGW induced by the PZT actuator propagates through the rail web. An artificial crack with the depth of 2 mm is placed (Figure 3). It is assumed that this crack would result in multiple scattering and reflections near the rail-crack interface. The baseline condition is firstly considered, where there are no defects located along the rail web. Then the dataset for testing is composed of 2 different scenarios: intact and crack conditions. It is worth noting that the test set is not used in the training process.

A total of 3 FBGs are installed onto the rail web surface, which are simultaneously demodulated in this experiment. Time-domain samples for all FBGs are presented in Figure 4. To avoid the error brought by the difference of FBGs deployed, the amplitude for each time when UGW signals are sampled, is normalized into the range of ±1. To construct a robust NARX model, both the target and exogenous inputs are required. Therefore, to this regard, the signals acquired by the middle FBG is determined as the target while the other 2 FBGs serve as the exogenous inputs to the NARX model.

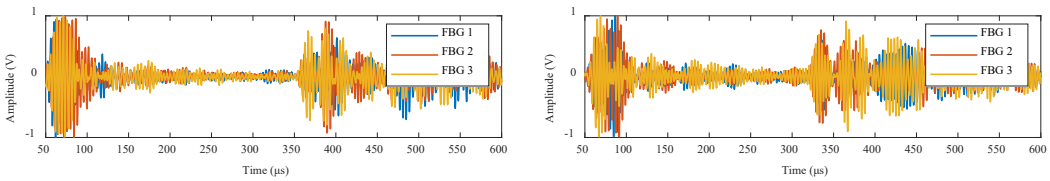

Figure 4. Sampled UGW signals sampled under the excitation frequency of 250 kHz in (a) Intact condition and (b) Crack condition.

RESULTS AND DISCUSSIONS

Instead of feeding the NARX model with the raw UGW data, Hilbert envelope is calculated first, as demonstrated in the following equation,

$$h(t) = \sum_{t}^{\infty} \frac{1}{f_s} a(t) e^{-j2\pi ft} \tag{4}$$

where f_s denotes the sampling frequency and $a(t)$ represents the instantaneous amplitude of the exponential formatted Hilbert transform of analytical signals. Then, the signal amplitudes are normalized to fit the range of 0 to 1. The actual and predicted Hilbert envelopes by NARX are presented in Figure 5. It can be clearly observed that better prediction results are achieved for intact condition.

To quantify the error distributions for both cases, the PDF histograms are shown in Figure 6. Compared to the PDF distribution of the crack condition, the error distribution for the intact condition clearly lies within the range of the baseline PDF distribution. With lower level of discreteness of the prediction error, the railway condition is more likely to be intact. Obvious peak shift and abnormal standard deviation can be intuitively observed in Figure 6(b), which proves that it is the existence of the artificial crack that contributes to the abnormal distribution of the NARX prediction error.

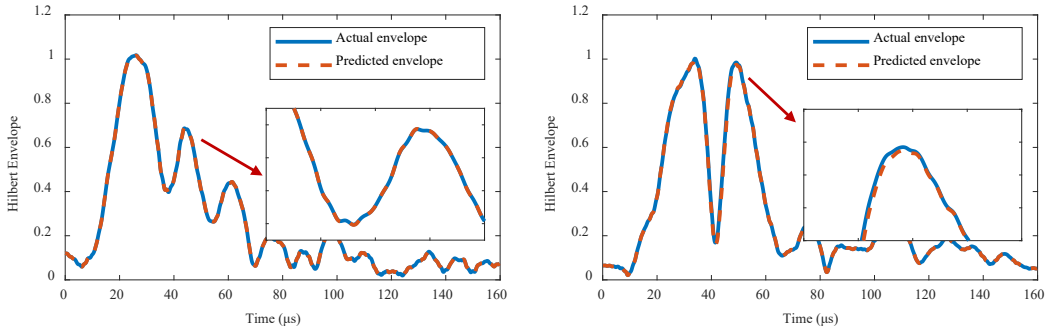

(a) (b)

Figure 5. Predictions of the NARX model with the UGW frequency of 250 kHz. (a) Intact; (b) Crack.

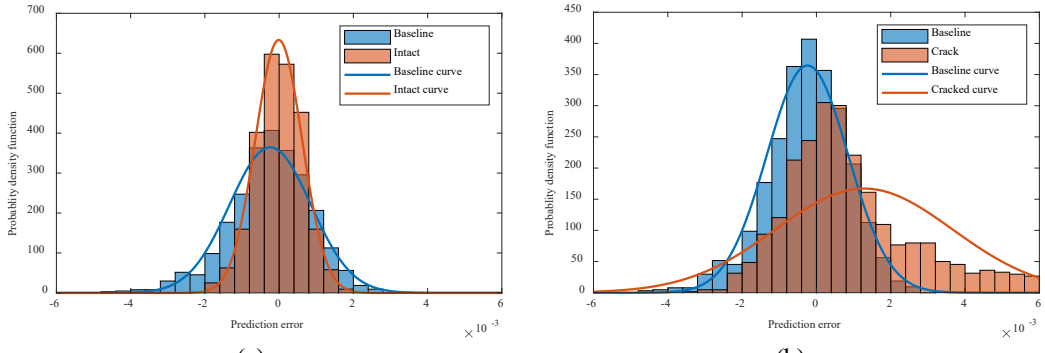

(a) (b)

Figure 6. PDFs of the prediction errors of (a) Intact condition and (b) Crack condition.

TABLE I. DAMAGE DETECTION RESULTS.

UGW frequency (kHz)	NARX training MSE	DSF thresholds	DSFs measured		Deviations (%)	
			Intact	Crack	Intact	Crack
150	1.93×10^{-5}	1.45	1.34	4.98	-7.59	**243.45**
200	4.52×10^{-5}	4.01	2.01	4.65	-49.9	**15.96**
250	3.91×10^{-5}	5.17	1.25	7.88	-75.8	**52.42**
300	5.56×10^{-5}	2.23	1.03	2.81	-53.81	**26.01**
350	6.97×10^{-5}	1.24	1.20	1.76	-0.03	**41.9**

Further validation is conducted in this paper, using various UGW excitation frequencies to detect the artificial crack, and the DSFs are calculated respectively. The damage detection results are shown in Table 1 below. For each UGW frequency, an individual NARX model is trained using the corresponding signals collected, and the training mean square error (MSE) values are quite low, indicating the excellent nonlinear fitting performance of NARX. The DSF thresholds are set based on the training results, using the average training error distribution. Then, the DSFs for both intact and crack conditions are calculated for comparison. The last 2 columns of the table show DSF deviations from the set thresholds are also presented in Table 1, where positive values denote that the prediction error distribution is more dispersed. For the intact condition, the DSFs for all UGW frequencies are lower than the thresholds. Whereas, for the crack condition, the DSFs are all significantly higher than the set thresholds. Therefore, it can be concluded that the chosen DSF can accurately represent the potential damaged status of the rail track.

CONCLUSIONS

In this paper, an FBG-based damage detection approach for railway tracks is proposed in conjunction with NARX neural networks. The DSF is composed of the key parameters extracted from the prediction error distribution of NARX models, to reveal the rail health status. For the experimental study in this paper, a defected railway track with an artificial crack with the width of 2 mm is configured. A hybrid sensing system composed of a PZT actuator and 3 FBG ultrasonic transducers is installed on the railway track. UGW signals are acquired and fed to the NARX model. The prediction results are presented, and the error distribution histograms are drawn to show the peak shifts and the deviation difference between the intact and crack rail conditions. DSFs are calculated with the excitation frequencies ranging from 150 kHz to 350 kHz. The damage detection results indicate that the proposed method can accurately detect the artificial crack on rail web. This NARX-based damage detection method is highly robust and has the potential to be massively utilized on railway systems.

REFERENCE

1. Loveday, P. W. 2012. “Guided wave inspection and monitoring of railway track,” Journal of Nondestructive Evaluation, 31(4):303–309.
2. Bombarda, D., G. M. Vitetta, and G. Ferrante. 2021. “Rail diagnostics based on ultrasonic guided waves: An overview,” Applied Sciences (Switzerland), 11(3):1–42.

3. Dirks, B., R. Enblom, A. Ekberg, and M. Berg. 2015. “The development of a crack propagation model for railway wheels and rails,” Fatigue Fract Eng Mater Struct, 38(12):1478–1491.
4. Sun, X., C. Guo, L. Yuan, Q. Kong, and Y. Ni. 2022. “Diffuse Ultrasonic Wave-Based Damage Detection of Railway Tracks Using PZT/FBG Hybrid Sensing System,” Sensors, 22(7), 2504.
5. Dang, D.-Z., C.-C. Lai, Y.-Q. Ni, Q. Zhao, B. Su, and Q.-F. Zhou. 2023. “Image Classification-Based Defect Detection of Railway Tracks Using Fiber Bragg Grating Ultrasonic Sensors,” *Appl. Sci.*, 13, 384.
6. Pang, D., Q. Sui, M. Wang, Y. Sai, R. Sun, and Y. Wang. 2018 “Acoustic Emission Source Localization System Using Fiber Bragg Grating Sensors and a Barycentric Coordinate-Based Algorithm,” J Sens, 2018, 9053284.
7. Wang, K., W. Cao, L. Xu, et al. 2020. “Diffuse ultrasonic wave-based structural health monitoring for railway turnouts,” Ultrasonics, 101, 106031.
8. Ramatlo, D. A., C. S. Long, P. W. Loveday, and D. N. Wilke. 2022. “Physics-based modelling and simulation of reverberating reflections in ultrasonic guided wave inspections applied to welded rail tracks,” J Sound Vib, 530,116914.
9. Wee, J., D. Hackney, P. Bradford, and K. Peters. 2017. “Bi-directional ultrasonic wave coupling to FBGs in continuously bonded optical fiber sensing,” *Appl Opt*, 56(25): 7262-7268.
10. Rautela, M., J. Senthilnath, J. Moll, and S. Gopalakrishnan. 2021. “Combined two-level damage identification strategy using ultrasonic guided waves and physical knowledge assisted machine learning,” Ultrasonics, 115, 106451.
11. Zhang, Z., H. Pan, X. Wang, and Z. Lin. 2022. “Deep Learning Empowered Structural Health Monitoring and Damage Diagnostics for Structures with Weldment via Decoding Ultrasonic Guided Wave,” Sensors, 22(14), 5390.
12. Yang, J. H., Q. Z. Kong, H. J. Liu, and H. Y. Peng. 2021. “Efficient Bayesian model class selection of vector autoregressive models for system identification,” *Struct Control Health Monit*, 28(9):2780.
13. Liu, A., L. Wang, L. Bornn, and C. Farrar. 2019. “Robust structural health monitoring under environmental and operational uncertainty with switching state-space autoregressive models,” *Struct Health Monit*, 18(2):435–453.
14. Azim, M. R. and M. Gül. 2019. “Damage detection of steel girder railway bridges utilizing operational vibration response,” *Struct Control Health Monit*, 26(11): 2447.
15. Umar, S., M. Vafaei, and S. C. Alih. 2021. “Sensor clustering-based approach for structural damage identification under ambient vibration,” *Autom Constr*, 121, 103433.